The Journal of the Acoustical Society of America

OCTOBER 01 1997

The usage of standard finite element codes for computation of dispersion relations in materials with periodic microstructure

M. Åberg; P. Gudmundson

Check for updates

J. Acoust. Soc. Am. 102, 2007–2013 (1997)
https://doi.org/10.1121/1.419652

View Online
Export Citation
CrossMark

27 February 2024 09:39:40

ASA
LEARN MORE
Advance your science and career as a member of the
Acoustical Society of America

ASA
ACOUSTICAL SOCIETY OF AMERICA

The usage of standard finite element codes for computation of dispersion relations in materials with periodic microstructure

M. Åberg and P. Gudmundson
Department of Solid Mechanics, Royal Institute of Technology, 100 44 Stockholm, Sweden

(Received 9 June 1996; accepted for publication 2 July 1997)

A method with which standard finite element programs can be used to compute dispersion relations in periodic composites is proposed. The method is applied to two composite microstructures: a two-phase laminate and a fiber composite. The dispersion relations computed for the laminate are compared with a known analytical solution and the agreement is very good. The dispersion relations computed for the fibrous composite are compared with an existing approximate model and experimental results from the literature. The agreement between the approximate model, the experiments, and the computations is very good in the wave guide case and satisfactory for the wave reflect case. © *1997 Acoustical Society of America.* [S0001-4966(97)04310-5]

PACS numbers: 43.20.Jr, 43.20.Gp, 43.20.Mv, 43.35.Cg [JEG]

INTRODUCTION

Structural materials are inhomogenous on small scales. In metals and ceramics the grain size usually defines the microstructural scale, and in composites it is the ply thickness, fiber dimension, or inclusion size that defines this scale. Generally, the inhomogeneous character of the material is ignored in engineering applications; the continuum hypothesis is assumed. The accuracy of this assumption is good if the stress and strain fields vary slowly compared to the microstructural length. In certain situations, however, this is not the case. Close to crack tips, for example, the stress and strain field vary strongly over microstructural lengths. Also, if the wavelength becomes sufficiently small, waves in inhomogeneous materials experience dispersion (i.e., phase and group velocities depend on the wavelength), as has been measured by Tauchert and Guzelsu,[1] Robinson and Leppelmeir,[2] Sutherland and Lingle,[3] and Kinra *et al.*[4] among others. In practice it is often impossible to analyze such problems using the conventional techniques of stress and strain calculations, therefore a number of simplified models, which take the microstructure into account, have been proposed.

One widely used technique is to smear out the effect of the microstructure and to calculate homogenized, or effective, properties as functions of the properties of the constituents. The so-called self-consistent scheme[5] has been developed and applied by Sabina *et al.* for the study of dispersion in materials with aligned and randomly oriented spheroids as inclusions.[6,7] Yang and Mal use a similar technique (the generalized self-consistent model) to study the dispersion in random fiber composites.[8] Random fiber composites have also been studied by Beltzer and Brauner by the use of the Kramers–Kronig relations.[9,10]

Another approach is to assume that the material is periodic and to apply an asymptotic multivariable expansion. One set of variables deals with the global stress and strain variations in the body, while the other set of variables take care of the rapid variations within a unit cell of the periodic material. The process is outlined in a number of texts; see, for example, Sanchez-Palencia and Zaouie,[11] Parton and Kudryavtsev,[12] Murakami *et al.*,[13] or Murakami and Hegemier.[14] To the authors' knowledge there are, however, relatively few examples of this procedure being carried out to the point where quantative comparisons with the results of other theories or experiments can be made.

Murakami *et al.* consider a laminate and derive approximate constitutive equations containing the microstructure. In order to assess the accuracy of the model, Murakami *et al.* calculate the dispersion relations resulting from their model and compare it with the exact results obtained by Sve.[15] Murakami and Hegemier use the same technique to model composites with hexagonally arranged fibers. Apart from the approximation involved with the expansion, another approximation is introduced based on a study by Murakami *et al.*[16] The hexagonally shaped unit cell boundary is approximated by a circle. From the resulting constitutive equations, the dispersion relation is calculated and compared with the experiments done by Tauchert and Guzelsu, and Sutherland and Lingle. Hence, it is unknown if the discrepancy between the calculated and the measured dispersion is due to the approximation made by the expansion and the simplified boundary or effects not accounted for, such as fiber-matrix slip or attenuation.

For the purpose of comparison there is, thus, a need for exact dispersion relations. In the one-dimensional case, i.e., a laminate, Sve and Delph *et al.* have obtained and discussed analytical solutions of dispersion relations.[17,18] For more complicated geometries one has to resort to numerical methods such as the finite element method.

The so-called stiffness method, which can be perceived as a finite element method, was used by Dong and Nelson to study wave motion in laminated plates.[19] Datta and coworkers used a refined version of the stiffness method to study wave motion in laminated plates and laminates.[20,21] Minagawa *et al.* use a mixed variational formulation and a new energy quotient to compute the dispersion relations for laminates, fiber composites with square fibers, and chequerboard composites, among others.[22–24] Naciri *et al.* use the finite element method to compute the dispersion and damping relations for a viscoelastic fibrous composite with square

27 February 2024 09:39:40

fibers.[25] The abovementioned finite element formulations result in eigenvalue problems with in general Hermitian stiffness and mass matrices. Nelson and Navi split the equations into real and imaginary parts and obtain a formulation which is used for computations of dispersion in a fiber composite with square fibers.[26] Orris and Petyt formulate a real eigenvalue problem using the fact that a complex eigenvalue problem with Hermitian matrices can be restated as a eigenvalue problem with real matrices at the expence of doubled matrix dimensions.[27] They then use this to compute dispersion in a periodically supported beam and a skin rib structure.

The methods mentioned above are, of course, generally applicable. It is, however, time consuming to apply them to a specific problem. Therefore it would be desirable to be able to use standard procedures included in most of the wide spread standard finite element codes for real valued field equations. Langlet *et al.* use a finite element code which handles complex fields called ATILA to compute dispersion,[28] however, most standard codes do not have this cabability. A nice thing with standard codes is that they automatically compute the stiffness and mass matrices and that constraints can easily be implemented; also the whole arsenal of pre- and post-processing that usually comes with these packages makes modeling and analysis of the results faster and more straightforward. This paper presents a procedure with which standard finite element programs for real valued fields can be used to compute dispersion relations. This method is then applied to two examples: a laminate and a fiber composite.

I. STATEMENT OF PROBLEM

A. Governing equations

Consider propagation of a harmonic wave in a periodic material. By periodic it is here meant that the material can be divided into finite-sized indentical, so-called periodic cells. Thus one single cell completely describes the material. The governing equations are

$$\sigma_{ij,j}=\rho\,\frac{\partial^2 u_i}{\partial t^2}, \tag{1}$$

$$\sigma_{ij}=C_{ijkl}\epsilon_{kl}, \tag{2}$$

and

$$\epsilon_{kl}=\tfrac{1}{2}(u_{k,l}+u_{l,k}). \tag{3}$$

Here, σ_{ij} is the stress tensor, ϵ_{kl} the strain tensor, u_i the displacement vector, C_{ijkl} the stiffness tensor, and ρ the density. In all tensor equations the usual summation convention is assumed and differentiation with respect to a Cartesian coordinate is denoted by a comma. Note that the stiffness and the density may both depend on position periodically.

Now look for solutions of the form

$$u_m(x_n,t)=U_m(x_n)e^{-i\omega t}, \tag{4}$$

where $U_m(x_n)$ is, in general, a complex valued function. As a consequence, the stresses and the strains will be given by

$$\sigma_{ij}(x_n,t)=\Sigma_{ij}(x_n)e^{-i\omega t} \tag{5}$$

and

$$\epsilon_{ij}(x_n,t)=E_{ij}(x_n)e^{-i\omega t}. \tag{6}$$

The equations of motion may now be written as

$$\Sigma_{ij,j}+\rho\omega^2 U_i=0, \tag{7}$$

$$\Sigma_{ij}=C_{ijkl}E_{kl}, \tag{8}$$

and

$$E_{kl}=\tfrac{1}{2}(U_{k,l}+U_{l,k}). \tag{9}$$

The periodic material is divided into periodic cells. Due to the periodicity the displacement vectors at equivalent points in different periodic cells are related through[29]

$$U_m(x_n)=U_m(x_n+l_n)e^{-ikn_j l_j}, \tag{10}$$

where k denotes the wave number, n_j the direction cosines of wave propagation, x_n a position vector, and l_n the vector connecting equivalent points in the periodic cells. From Eqs. (8) and (9) it follows that the stresses in the points under consideration satisfy an equivalent periodicity relation, thus

$$\Sigma_{ij}(x_n)=\Sigma_{ij}(x_n+l_n)e^{-ikn_j l_j}. \tag{11}$$

A single periodic cell is now considered. For each point on the boundary of the cell there exists an equivalent periodic point for which relations (10) and (11) are valid. For corner points of the cell, in particular, there exists more than one equivalent periodic point. Excluding for a moment the singular case of corner points, the pair of equivalent points on the boundary of the periodic cell have outward normal vectors in opposite directions. Hence the traction vectors, S_m, are defined by

$$S_m(x_n)=\Sigma_{mj}(x_n)n_j \tag{12}$$

and satisfy the following periodicity equation:

$$S_m(x_n)\mp -S_m(x_n+l_n)e^{-ikn_j l_j}. \tag{13}$$

Thus the boundary conditions on the outer surfaces of the periodic cell are given by Eqs. (10) and (13). Because very few of the standard finite element programs in solid mechanics handle complex valued displacements, the displacement and other fields are split into real and imaginary parts. That is,

$$U_m(x_n)=U_m^{\mathrm{Re}}(x_n)+iU_m^{\mathrm{Im}}(x_n), \tag{14}$$

$$S_m(x_n)=S_m^{\mathrm{Re}}(x_n)+iS_m^{\mathrm{Im}}(x_n). \tag{15}$$

In doing this, Eq. (7) splits into the equations,

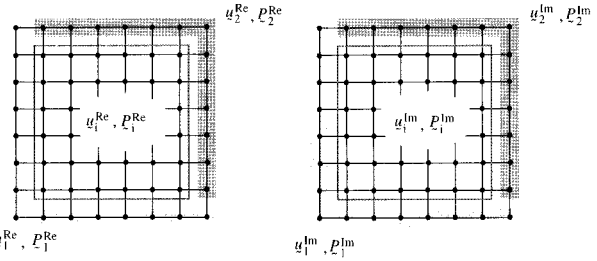

FIG. 1. Principle of the division and labeling of nodal displacements and nodal forces.

27 February 2024 09:39:40

$$\Sigma_{ij,j}^{\mathrm{Re}}+p\omega^2 U_i^{\mathrm{Re}}=0,$$
$$\Sigma_{ij,j}^{\mathrm{Im}}+p\omega^2 U_i^{\mathrm{Im}}=0, \tag{16}$$

for the real and imaginary parts, respectively. Boundary conditions (10) and (13) transform into

$$U_m^{\mathrm{Re}}(x_n)=U_m^{\mathrm{Re}}(x_n+l_n)\cos(kn_jl_j)+U_m^{\mathrm{Im}}(x_n+l_n)\sin(kn_jl_j), \tag{17}$$

$$U_m^{\mathrm{Im}}(x_n)=U_m^{\mathrm{Im}}(x_n+l_n)\cos(kn_jl_j)-U_m^{\mathrm{Re}}(x_n+l_n)\sin(kn_jl_j)$$

and

$$S_m^{\mathrm{Re}}(x_n+l_n)=-S_m^{\mathrm{Re}}(x_n)\cos(kn_jl_j)+S_m^{\mathrm{Im}}(x_n)\sin(kn_jl_j),$$
$$S_m^{\mathrm{Im}}(x_n+l_n)=-S_m^{\mathrm{Im}}(x_n)\cos(kn_jl_j)-S_m^{\mathrm{Re}}(x_n)\sin(kn_jl_j). \tag{18}$$

B. Finite element formulation

Since the real and imaginary parts are uncoupled in Eq. (16), it is possible to solve the eigenvalue problem defined by Eqs. (16), (17), and (18) using two identical, unit cell shaped, finite element meshes—one for the real part and one for the imaginary part. If the boundaries of the two meshes are coupled by the displacement boundary conditions in Eq. (17), the boundary conditions for the tractions are fulfilled automatically due to the way that most standard finite element codes implement condition (17).

In order to highlight this, consider the two identical two-dimensional meshes in Fig. 1 representing a quadratic unit cell. The finite element formulation of Eq. (16) is

$$\left(\begin{bmatrix}[K] & 0\\ 0 & [K]\end{bmatrix}-\omega^2\begin{bmatrix}[M] & 0\\ 0 & [M]\end{bmatrix}\right)\begin{bmatrix}\mathbf{u}_i^{\mathrm{Re}}\\ \mathbf{u}_1^{\mathrm{Re}}\\ \mathbf{u}_2^{\mathrm{Re}}\\ \mathbf{u}_i^{\mathrm{Im}}\\ \mathbf{u}_1^{\mathrm{Im}}\\ \mathbf{u}_2^{\mathrm{Im}}\end{bmatrix}=\begin{bmatrix}\mathbf{P}_i^{\mathrm{Re}}\\ \mathbf{P}_1^{\mathrm{Re}}\\ \mathbf{P}_2^{\mathrm{Re}}\\ \mathbf{P}_i^{\mathrm{Im}}\\ \mathbf{P}_1^{\mathrm{Im}}\\ \mathbf{P}_2^{\mathrm{Im}}\end{bmatrix}. \tag{19}$$

Here the vector $\mathbf{u}^{\mathrm{Re}}$, the real part of the displacement, is partioned into $\mathbf{u}_i^{\mathrm{Re}}$, $\mathbf{u}_1^{\mathrm{Re}}$, and $\mathbf{u}_2^{\mathrm{Re}}$ denoting the internal nodes, the nodes of set 1, and the nodes of set 2, respectively. The real parts of the corresponding nodal forces are labeled $\mathbf{P}_i^{\mathrm{Re}}$, $\mathbf{P}_1^{\mathrm{Re}}$, and $\mathbf{P}_2^{\mathrm{Re}}$. The imaginary counterparts have the superscript ''Im'' instead of ''Re.'' The submatrices $[K]$ and $[M]$ are the stiffness and mass matrices, of a single mesh, respectively. Boundary conditions (17) have the following appearance:

$$\begin{bmatrix}\mathbf{u}_i^{\mathrm{Re}}\\ \mathbf{u}_1^{\mathrm{Re}}\\ \mathbf{u}_2^{\mathrm{Re}}\\ \mathbf{u}_i^{\mathrm{Im}}\\ \mathbf{u}_1^{\mathrm{Im}}\\ \mathbf{u}_2^{\mathrm{Im}}\end{bmatrix}=[Q]\begin{bmatrix}\mathbf{u}_i^{\mathrm{Re}}\\ \mathbf{u}_2^{\mathrm{Re}}\\ \mathbf{u}_i^{\mathrm{Im}}\\ \mathbf{u}_2^{\mathrm{Im}}\end{bmatrix}. \tag{20}$$

The constraint matrix $[Q]$ can be schematically written as

$$[Q]=\begin{bmatrix}[I] & 0 & 0 & 0\\ 0 & [C] & 0 & [S]\\ 0 & [I] & 0 & 0\\ 0 & 0 & [I] & 0\\ 0 & -[S] & 0 & [C]\\ 0 & 0 & 0 & [I]\end{bmatrix}, \tag{21}$$

where $[C]$ and $[S]$ are diagonal block matrices containing the sine and cosine factors of Eq. (17). Substitution of Eq. (20) into (19) and premultiplication by $[Q]^T$ yields the following system of equations:

$$[Q]^T\left(\begin{bmatrix}[K] & 0\\ 0 & [K]\end{bmatrix}-\omega^2\begin{bmatrix}[M] & 0\\ 0 & [M]\end{bmatrix}\right)[Q]\begin{bmatrix}\mathbf{u}_i^{\mathrm{Re}}\\ \mathbf{u}_2^{\mathrm{Re}}\\ \mathbf{u}_i^{\mathrm{Im}}\\ \mathbf{u}_2^{\mathrm{Im}}\end{bmatrix}=\begin{bmatrix}\mathbf{P}_i^{\mathrm{Re}}\\ [C]\mathbf{P}_1^{\mathrm{Re}}+\mathbf{P}_2^{\mathrm{Re}}-[S]\mathbf{P}_1^{\mathrm{Im}}\\ \mathbf{P}_i^{\mathrm{Im}}\\ [C]\mathbf{P}_1^{\mathrm{Im}}+\mathbf{P}_2^{\mathrm{Im}}+[S]\mathbf{P}_1^{\mathrm{Re}}\end{bmatrix}. \tag{22}$$

When a standard finite element code computes the eigenfrequencies and eigenmodes, the vector on the right-hand side of Eq. (22) is set to zero. In Eq. (22) this corresponds to an absence of body forces on the internal node set and the fulfillment of the traction boundary conditions in Eq. (18). In other words, the boundary conditions of Eq. (18) are automatically fulfilled if Eq. (17) is fulfilled.

Thus by having two identical finite element meshes and implementing the constraints of Eq. (17), the eigenfrequencies ω, which can be shown to be double eigenvalues, can be computed for any given wave number, k, and wave direction, n_j. This procedure makes it possible to compute the dispersion relation for the periodic material.

27 February 2024 09:39:40

C. Phase and group velocity

When the dispersion relation is known two velocities may be calculated—the phase and group velocities. The phase velocity, c_p, is the speed with which a point of constant phase moves through the medium. If the eigenfrequency is known for a given wave number the components of the phase velocity is calculated according to

$$c_{pi}=\frac{\omega}{k}\,n_i\,. \tag{23}$$

The group velocity is the speed at which energy travels through the medium. The components of the group velocity vector, c_{gi}, are found from

$$c_{gi}=\frac{\partial\omega}{\partial k_i}. \tag{24}$$

Here, $k_i=kn_i$ are the components of the wave vector. Note that the direction of the group velocity is not necessarily the same as the direction of wave propagation. Following Kline an expression for the group velocity in terms of boundary displacements and boundary forces may be derived.[30] Begin by defining

$$\Psi_j=\frac{1}{T}\int_0^T \dot{u}_i(x_m,t)\sigma_{ij}(x_m,t)dt. \tag{25}$$

Here, a dot denotes derivation with respect to time and T is the period of the plane wave. Evaluated, this becomes

$$\Psi_j=\frac{\omega}{2}\,(U_i^{\mathrm{Re}}\Sigma_{ij}^{\mathrm{Im}}-U_i^{\mathrm{Im}}\Sigma_{ij}^{\mathrm{Re}}), \tag{26}$$

where U_i^{Re} and U_i^{Im} are defined as in Eqs. (4) and (14), and $\Sigma_{ij}^{\mathrm{Re}}$ and $\Sigma_{ij}^{\mathrm{Im}}$ are defined by Eq. (5) and the relation

$$\Sigma_{ij}(x_i)=\Sigma_{ij}^{\mathrm{Re}}(x_i)+i\Sigma_{ij}^{\mathrm{Im}}(x_i). \tag{27}$$

The time average of the total energy density, E, in a point can be written as

$$E=\frac{1}{T}\int_0^T \rho\dot{u}_i(x_m,t)\dot{u}_i(x_m,t)dt. \tag{28}$$

With the notation of Eqs. (4) and (14) this becomes

$$E=\frac{\omega^2}{2}\,\rho[U_i^{\mathrm{Re}}U_i^{\mathrm{Re}}+U_i^{\mathrm{Im}}U_i^{\mathrm{Im}}]. \tag{29}$$

Now the average power P per unit area with normal vector n_j may be written in terms of Ψ_j as

$$P=\frac{1}{\Gamma}\int_\Gamma \Psi_j n_j\,d\Gamma, \tag{30}$$

where Γ is a representative surface element. The average energy in a representative volume may be expressed as

$$E=\frac{1}{V}\int_V E\,dV, \tag{31}$$

where V is the representative volume.

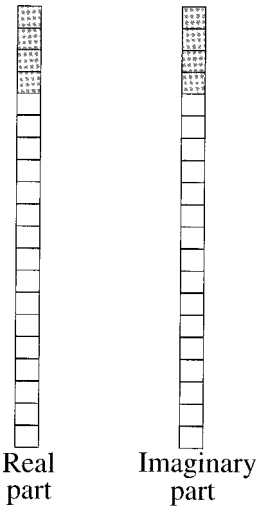

FIG. 2. The simple meshes used for the laminate. The shadowed elements denote material 1 and the unshadowed material 2.

For a periodic material the representative volume, V, and surface, Γ, may be defined from a single periodic cell. The component of the group velocity in the normal direction of Γ, n_i, then takes the value

$$c_{gi}n_i=\frac{V\int_\Gamma(U_i^{\mathrm{Re}}S_i^{\mathrm{Im}}-U_i^{\mathrm{Im}}S_i^{\mathrm{Re}})d\Gamma}{\omega\Gamma\int_V\rho[U_i^{\mathrm{Re}}U_i^{\mathrm{Re}}+U_i^{\mathrm{Im}}U_i^{\mathrm{Im}}]dV}. \tag{32}$$

The right-hand side of Eq. (32) gives the ratio between average energy flux through the unit cell in the direction of the normal of the surface Γ and average total energy in the unit cell. Equation (32) is suitable for finite element computations. The integrals are then exchanged by sums, and U_i and S_i are taken as the nodal displacements and nodal forces, respectively.

II. EXAMPLES

A. Laminate

In order to certify the above presented method, dispersion relations for an elastic two phase laminate were computed using the standard finite element program ABAQUS[31] and compared with the exact solution due to Sve. In the case of laminates the meshes were very simple. Two rows of 20 square eight-node biquadratic plain strain elements—one row for the real and imaginary parts, respectively—were used (see Fig. 2). In order to avoid false eigenfrequencies, the model should be as thin as possible in the direction of translation symmetry. In this case only one row of elements should be used. The value of the wave number, k, and the direction of wave propagation, n_i, was given and ABAQUS was used to compute the eigenfrequencies. The values of the material and geometric parameters used are found in Table I.

TABLE I. Material and geometric properties of the laminate. The density is denoted ρ, the relative thickness of a ply is denoted D, and λ and μ are Lamé's constants.

ρ_2/ρ_1	μ_2/μ_1	λ_1/μ_1	λ_2/μ_1	$D_1/(D_1+D_2)$	$D_2/(D_1+D_2)$
3	50	2.33	75	0.2	0.8

27 February 2024 09:39:40

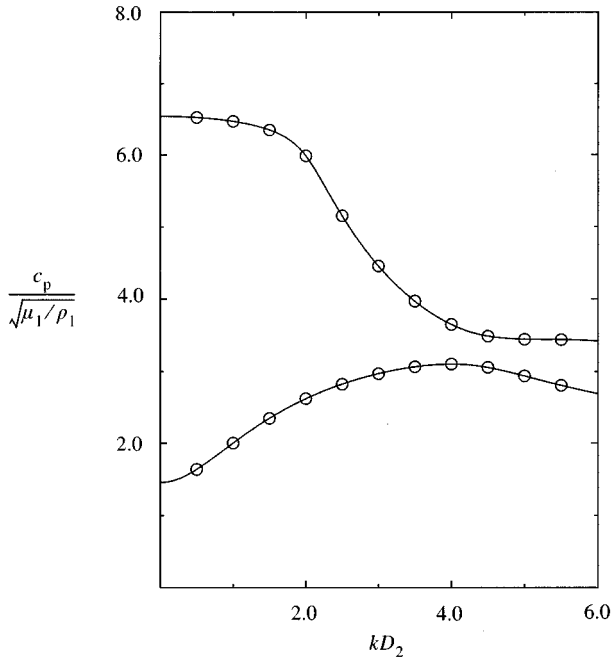

FIG. 3. Dimensionless phase velocity as functions of dimensionless wave number for the laminate. The wave vector and the normal of the plies make a 75-deg angle. The solid line is due to Sve (Ref. 15) and the circles (○) are the computed values.

Subscripts 1 and 2 refer to material 1 and 2, respectively. The density is denoted ρ, the relative thickness of a ply is denoted D, and λ and μ are Lamé's constants. As an example the results for wave propagation where the wave vector and the normal of the plies make a 75 degree angle is presented in Fig. 3. A dimensionless phase velocity is plotted as a function of a dimensionless wave number. The solid line is the relation found by Sve and the circles are points computed by use of ABAQUS. The difference between calculated and computed values was less than 0.1%. The comparison was made for several other wave vector angles and in all cases the agreement was equally good.

B. Hexagonal fiber composite

In order to assess the accuracy of Murakami and Hegemier's model, finite element computations were made on a hexagonally arranged fiber composite. The parameter values used correspond to the epoxy boron composite used by Murakami and Hegemier and are given in Table II. The unit cell was modeled using 416 eight-node brick elements in each mesh. The mesh used is shown in Fig. 4 (remember that two meshes have to be used although only one mesh is shown). Note that only one layer of elements is used in the direction

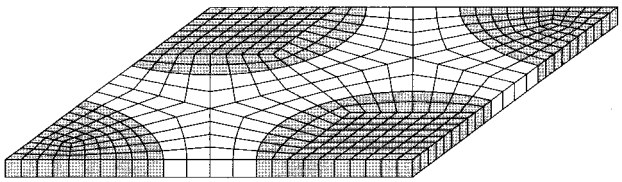

FIG. 4. The finite element mesh used for the fibrous composite.

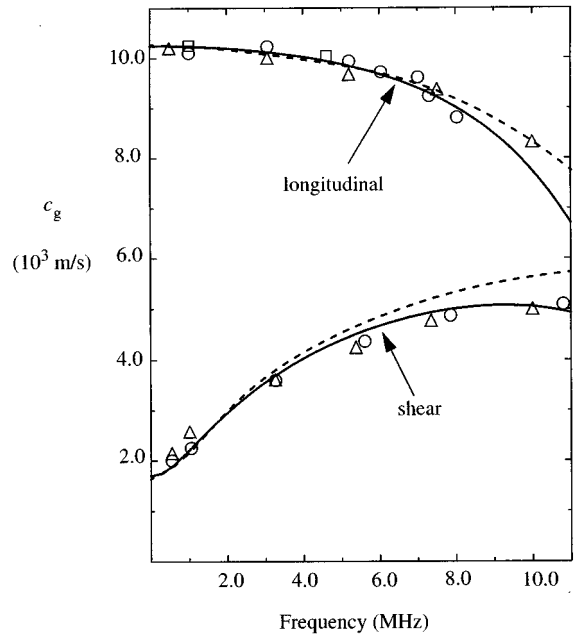

FIG. 5. Group velocity of wave guide modes as functions of frequency for the fibrous composite. Solid curve, computed values. Dashed curve, Murakami and Hegemier (Ref. 14). Symbols, Tauchert and Guzelsu (Ref. 1).

of translation symmetry. In order to check the convergence of the computed eigenfrequencies a few computations were also done for a mesh with roughly four times as many elements. The difference in group velocity between the coarser mesh that was used and the finer mesh was roughly one percent. Figure 5 shows a comparison between the computed dispersion relation (the solid curve), experiments done by Tauchert and Guzelsu (the symbols are the ones used in their work), and the dispersion relations due to Murakami and Hegemier (the dashed curve) for the so-called waveguide

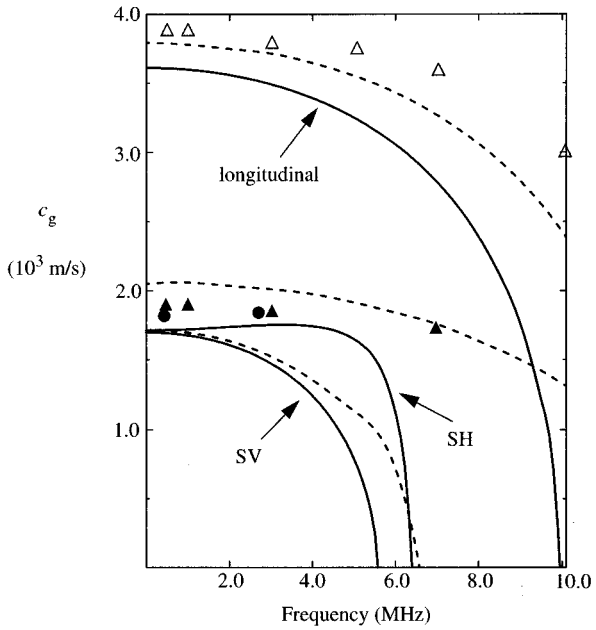

FIG. 6. Group velocity of wave reflect modes as functions of frequency for the fibrous composite. Solid curve, computed values. Dashed curve, Murakami and Hegemier (Ref. 14). Symbols, Tauchert and Guzelsu (Ref. 1).

27 February 2024 09:39:40

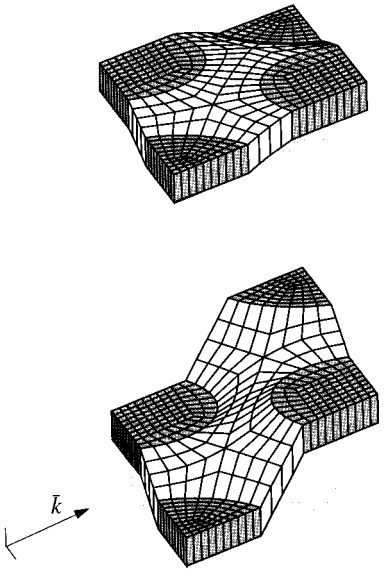

FIG. 7. An example of output from post-processing. The first mode (*SV*) for the wave reflect case at a frequency of 2 MHz.

case, i.e., the wave vector is directed along the fibers. Figure 6 shows a comparison for the wave reflect case, i.e., the wave vector is directed normal to the fibers.

A minor complication with ABAQUS is that the program does not include the mass matrix in Eq. (19) when asked to compute the constraint forces from the eigenmodes. Therefore Eq. (32) could not be used and the differentiation according to Eq. (24) had to be done numerically. Since the material is symmetric with respect to the direction of the wave vector in the two cases considered, the group velocity and the wave vector have the same direction. The group velocity is then calculated according to

$$c_{gi}=\frac{\partial \omega}{\partial k}\, n_i\,, \tag{33}$$

where k is the magnitude of the wave vector and n_i are the direction cosines of the wave vector. The derivation was done numerically by the central difference scheme.

Figure 7 shows an example of the output that may be obtained from a post-processor. The first eigenmode for the wave reflect case and a frequency of 2 MHz is showed. The shading, corresponding to a light source directly above the model, has been added for clearity.

III. DISCUSSION AND CONCLUSIONS

The good agreement between computed values and the exact solution (Fig. 3) in the laminate example certifies that the method presented will work for more complicated geometries as well.

TABLE II. Properties of the boron/epoxy fibrous composite.

	E-modulus E	Poisson's ratio ν	Mass density ρ	Volume fraction D
Boron	379.2 GPa	0.18	2682 kg/m^3	0.54
Epoxy	5.033 GPa	0.40	1261 kg/m^3	0.46

The results for the fibrous composite are shown in Figs. 5 and 6. The two lowest wave guide modes are shown in Fig. 5. The lowest mode corresponds to a shear wave and the other mode is a longitudinal wave. The model of Murakami and Hegemier is quite successful in predicting the behavior up to about 6 MHz, after which the model overestimates the group velocities. The experimental values lie closer to the computed group velocities, at least for the shear wave mode. In Fig. 6 the three lowest wave reflect modes are shown. The two lowest modes correspond to shear waves and the third mode is a longitudinal wave. The agreement between the model of Murakami and Hegemier and the presented computation is not as good as in the wave guide case. In fact, the model of Murakami and Hegemier and the computed values do not agree in the static limit (i.e., for $k=0$, which corresponds to zero frequency). Also, the model of Murakami and Hegemier predicts that the lowest mode is a horizontally polarized shear wave (*SH* mode) and that the next mode is a vertically polarized shear wave (*SV* mode). The computations, however, show that it is the other way around. Figure 7 shows the first eigenmode for the wave reflect case; as can be seen this is an *SV* mode. The experiments do not fit the computations as nicely in the wave reflect case as in the wave guide case, but the qualitative behavior is approximately the same. Tauchert and Guzelsu state that the lowest experimental group velocities were traveling *SH* waves, and the computed *SH*-wave group velocities lie closest to those points. The discrepancy between computed and experimental values could partly be due to the fact that the fibrous composite used by Tauchert and Guzelsu was not transversely isotropic, but rather it was a tetragonal material. It is notable that the model of Murakami and Hegemier in this case also overestimates the group velocities. It seems that the model by Murakami and Hegemier is more successful in predicting the behavior of the material for waves in the fiber direction than the behavior for waves normal to the fibers.

Based on the agreement between computations and theory for the laminate and the reasonable results for the fibrous composite, it is concluded that the method presented is useful for computations of dispersion relations for periodic materials. It should also work for other types of periodic structures such as plates and pipes with stiffeners.

ACKNOWLEDGMENTS

Financial support from the Swedish Research Council for Engineering Sciences (TFR) is gratefully acknowledged.

[1] T. R. Tauchert and A. N. Guzelsu, ''An experimental study of dispersion of stress waves in a fiber-reinforced composite,'' J. Appl. Mech. **39**, 98–102 (1972).
[2] C. W. Robinson and G. W. Leppelmeier, ''Experimental verification of dispersion relations for layered composites,'' J. Appl. Mech. **41**, 89–91 (1974).
[3] H. J. Sutherland and R. Lingle, ''Geometric dispersion of acoustic waves by a fibrous composite,'' J. Compos. Mater. **6**, 490–502 (1972).
[4] V. K. Kinra and V. Dayal, ''Acoustic methods of evaluating elastic properties or, will the real Young's modulus please stand up?,'' in *Manual on Experimental Methods for Mechanical Testing of Composites*, edited by R. L. Pendleton and M. E. Tuttle (Elsevier Applied Science, London, 1989), Sec. VA, pp. 97–103.

27 February 2024 09:39:40

[5] R. M. Christensen, *Mechanics of Composite Materials* (Krieger, Malabar, FL, 1991), p. 59.
[6] F. J. Sabina, V. P. Smyshlyaev, and J. R. Willis, ''Self-consistent analysis of waves in a matrix-inclusion composite—I. Aligned spheroidal inclusions,'' J. Mech. Phys. Solids **41**, 1573–1588 (1993).
[7] V. P. Smyshlyaev, J. R. Willis, and F. J. Sabina, ''Self-consistent analysis of waves in a matrix-inclusion composite—II. Randomly oriented spheroidal inclusions,'' J. Mech. Phys. Solids **41**, 1589–1598 (1993).
[8] R. Yang and A. K. Mal, ''Multiple scattering of elastic waves in a fiber-reinforced composite,'' J. Mech. Phys. Solids **42**, 1945–1968 (1994).
[9] A. I. Beltzer and N. Brauner, ''SH waves of an arbitrary frequency in random fibrous composites via the $K-K$ relations,'' J. Mech. Phys. Solids **33**, 471–487 (1985).
[10] A. I. Beltzer and N. Brauner, ''The dynamic response of random composites by causal differential method,'' Mech. Mater. **6**, 337–345 (1987).
[11] E. Sanchez-Palencia and A. Zaouie, *Homogenization Techniques for Composite Media*, Lecture Notes in Physics No. 272 (Springer-Verlag, Berlin, 1986).
[12] V. Z. Parton and B. A. Kudryavtsev, *Engineering Mechanics of Composite Structures* (CRC, Boca Raton, 1993).
[13] H. Murakami, A. Maewal, and G. A. Hegemier, ''A mixture theory with a director for linear elastodynamics of periodically laminated media,'' Int. J. Solids Struct. **17**, 155–173 (1981).
[14] H. Murakami and G. A. Hegemier, ''A mixture model for unidirectionally fiber-reinforced composites,'' J. Appl. Mech. **53**, 765–773 (1986).
[15] C. Sve, ''Time-harmonic waves traveling obliquely in a periodic laminated medium,'' J. Appl. Mech. **38**, 477–482 (1971).
[16] H. Murakami, A. Maewal, and G. A. Hegemier, ''Mixture theory for longitudinal wave propagation in unidirectional composites with cylindrical fibers of arbitrary cross section—II,'' Int. J. Solids Struct. **15**, 335–357 (1979).
[17] T. J. Delph, G. Hermann, and R. K. Kaul, ''Harmonic wave propagation in a periodically layered, infinite elastic body: Plane strain, analytical results[1],'' J. Appl. Mech. **46**, 113–119 (1979).
[18] T. J. Delph, G. Hermann, and R. K. Kaul, ''Harmonic wave propagation in a periodically layered, infinite elastic body: Plane strain, numerical results[2],'' J. Appl. Mech. **47**, 531–537 (1980).
[19] S. B. Dong and R. B. Nelson, ''On natural vibrations and waves in laminated orthotropic plates,'' J. Appl. Mech. **39**, 739–745 (1972).
[20] A. H. Shah and S. K. Datta, ''Harmonic waves in a periodically laminated medium,'' Int. J. Solids Struct. **18**, 397–410 (1982).
[21] S. K. Datta, A. H. Shah, R. L. Bratton, and T. Chakraborty, ''Wave propagation in laminated composite plates,'' J. Acoust. Soc. Am. **83**, 2020–2026 (1988).
[22] S. Minagawa and S. Nemat-Nasser, ''On harmonic waves in layered composites,'' J. Appl. Mech. **44**, 689–695 (1977).
[23] S. Minagawa, S. Nemat-Nasser, and M. Yamada, ''Finite element analysis of harmonic waves in layered and fiber-reinforced composites,'' Int. J. Numer. Methods Eng. **17**, 1335–1353 (1981).
[24] S. Minagawa, S. Nemat-Nasser, and M. Yamada, ''Dispersion of waves in two-dimensional layered, fiber-reinforced, and other elastic composites,'' Comput. Struct. **19**, 119–128 (1984).
[25] T. Naciri, P. Navi, and A. Ehrlacher, ''Harmonic wave propagation in viscoelastic heterogeneous materials. Part I: Dispersion and damping relations,'' Mech. Mater. **18**, 313–333 (1994).
[26] R. B. Nelson and P. Navi, ''Harmonic wave propagation in composite materials,'' J. Acoust. Soc. Am. **57**, 773–781 (1975).
[27] R. M. Orris and M. Petyt, ''A finite element study of harmonic wave propagation in periodic structures,'' J. Sound Vib. **33**, 223–236 (1974).
[28] P. Langlet, A.-C. Hladky-Hennion, and J.-N. Decarpigny, ''Analysis of the propagation of plane acoustic waves in passive periodic materials us ing the finite element method,'' J. Acoust. Soc. Am. **98**, 2792–2800 (1995).
[29] L. Brillouin, *Wave Propagation in Periodic Structures* (Dover, New York, 1953).
[30] R. A. Kline, *Nondestructive Characterization of Composite Media* (Technomic, Lancaster, 1992).
[31] *ABAQUS User's Manual version 5.4* (Hibbit, Karlsson, and Sorensen, Inc., Pawtucket, RI, 1994).

27 February 2024 09:39:40